

Isolation and Structural Characterization of Two Very Large, and Largely Empty, Endohedral Fullerenes: $\text{Tm}@C_{3V}\text{-C}_{94}$ and $\text{Ca}@C_{3V}\text{-C}_{94}$

Yuliang Che,[†] Hua Yang,[†] Zhimin Wang,[†] Hongxiao Jin,[†] Ziyang Liu,^{*,†} Chunxin Lu,[†] Tianming Zuo,[‡] Harry C. Dorn,^{*,‡} Christine M. Beavers,[§] Marilyn M. Olmstead,^{*,§} and Alan L. Balch^{*,§}

[†]Department of Chemistry, Zhejiang University, Hangzhou 310027, China, [‡]Department of Chemistry, Virginia Polytechnic Institute and State University, Blacksburg, Virginia 24061, and [§]Department of Chemistry, University of California, Davis, One Shields Avenue, Davis, California 95616

Received February 17, 2009

The structures of two newly synthesized endohedral fullerenes, $\text{Tm}@C_{3V}\text{-C}_{94}$ and $\text{Ca}@C_{3V}\text{-C}_{94}$, have been determined by single crystal X-ray diffraction on samples cocrystallized with Ni^{II} (octaethylporphyrin). Both compounds exhibit the same cage geometry and conform to the isolated pentagon rule (IPR). The metal ions within these rather large cages are localized near one end and along the C_3 axis. While the calcium ion is situated over a C–C bond at a 6:6 ring junction, the thulium ion is positioned above a six-membered ring of the fullerene.

Introduction

The chemistry of fullerenes is not confined to C_{60} and C_{70} but also includes much larger cages. Fullerenes are generally prepared by vaporization of graphite in an electric arc in a low-pressure atmosphere.¹ Under these conditions, C_{60} and C_{70} are the dominant products. However, larger, all-carbon clusters with even numbers of atoms up to C_{500} have been successfully extracted from the carbon soot produced by the arcing process.^{2,3} Empty fullerene cages obey the isolated pentagon rule (IPR), which requires that each of the twelve pentagons in the carbon cage be surrounded by hexagons.⁴ For C_{60} there is only one isomer that satisfies the IPR, and a similar situation pertains for C_{70} . But as the size of the fullerene cage increases, the possibilities for the existence of multiple isomers also increase. Thus, for C_{80} there are 7 isomeric structures that conform to the IPR, for C_{90} there are 46 such isomers and for C_{100} there are 450 possible isomers.

Endohedral fullerenes with carbon cage sizes of 80, 82, and 84 atoms have received extensive study in recent years.⁵ With the development of endohedral fullerenes encapsulating M_3N units, of which $\text{Sc}_3\text{N}@I_h\text{-C}_{80}$ is the prototypical

example,⁶ there has been a concerted effort to determine the range of sizes of carbon cages that can surround these M_3N units.^{7–9} Particular attention has been paid to the effect of metal ion size in determining the cage size for endohedral fullerenes of the $M_3N@C_{2n}$ class. In that regard, Echegoyen and co-workers have observed that large metal ions like cerium favor the formation of large cages with species as large as $\text{Ce}_3\text{N}@C_{104}$ detectable by mass spectroscopy.^{10,11} Some of the largest endohedral fullerenes to be fully structurally characterized by single crystal X-ray diffraction, $\text{Tb}_3\text{N}@D_2(35)\text{-C}_{88}$ and $\text{Tb}_3\text{N}@D_3(19)\text{-C}_{86}$, belong to this $M_3N@C_{2n}$ class.

While considerable efforts have gone into expanding the number of endohedral fullerenes of the $M_3N@C_{2n}$ class, there also has been significant development in expanding the range and sizes of endohedrals containing other atomic groupings as well. Recently, the detection of an extensive family of digadolinium endohedrals that extends from Gd_2C_{90} to $\text{Gd}_2\text{C}_{124}$ has been reported and the structure of one of these, $\text{Gd}_2\text{C}_2@D_3(85)\text{-C}_{92}$, has been established crystallographically.¹² Prior to the work reported here,

*To whom correspondence should be addressed. E-mail: zyliu@zju.edu.cn (Z.L.), hdorn@vt.edu (H.C.D.), mmolmstead@ucdavis.edu (M.M.O.), albalch@ucdavis.edu (A.L.B.).

(1) Krätschmer, W.; Lamb, L. D.; Fostiropoulos, K.; Huffman, D. R. *Nature* 1990, 347, 354.

(2) Shinohara, H.; Saito, H.; Saito, Y.; Izuoka, A.; Sugawara, T.; Ito, H.; Sakurai, T.; Matsuo, T. *Rapid Commun. Mass Spectrom.* 1992, 6, 413.

(3) Beer, F.; Gugel, A.; Martin, K.; Rader, J.; Mullen, K. *J. Mater. Chem.* 1997, 7, 1327.

(4) Fowler, P. W.; Manolopoulos, D. E. *An Atlas of Fullerenes*; Clarendon Press: Oxford, 1995.

(5) *Endofullerenes: A New Family of Carbon Clusters*; Akasaka, T., Nagase, S., Eds.; Springer: New York, 2002.

(6) Stevenson, S.; Rice, G.; Glass, T.; Harich, K.; Cromer, F.; Jordan, M. R.; Craft, J.; Hadju, E.; Bible, R.; Olmstead, M. M.; Maitra, K.; Fisher, A. J.; Balch, A. L.; Dorn, H. C. *Nature* 1999, 401, 55.

(7) Yang, S.; Dunsch, L. *J. Phys. Chem. B* 2005, 109, 12320.

(8) Yang, S.; Dunsch, L. *Chem.—Eur. J.* 2006, 12, 413.

(9) Zuo, T.; Beavers, C. M.; Duchamp, J. C.; Campbell, A.; Dorn, H. C.; Olmstead, M. M.; Balch, A. L. *J. Am. Chem. Soc.* 2007, 129, 2035.

(10) Chaur, M. N.; Melin, F.; Elliott, B.; Kumbhar, A.; Athans, A. J.; Echegoyen, L. *Chem.—Eur. J.* 2008, 14, 4594.

(11) Melin, F.; Chaur, M. N.; Engmann, S.; Elliott, B.; Kumbhar, A.; Athans, A. J.; Echegoyen, L. *Angew. Chem., Int. Ed.* 2007, 46, 9032.

(12) Yang, H.; Lu, C.; Liu, Z.; Jin, H.; Che, Y.; Olmstead, M. M.; Balch, A. L. *J. Am. Chem. Soc.* 2008, 130, 17296.

Article

$\text{Gd}_2\text{C}_2@D_3(85)\text{-C}_{92}$ involved the largest fullerene cage whose structure has been determined by single crystal X-ray diffraction.

There also has been significant development in detecting large endohedrals containing just a single metal ion. For example, several calcium containing endohedral fullerenes have been isolated including $\text{Ca}@C_{60}$,¹³ $\text{Ca}@C_{72}$,¹⁴ $\text{Ca}@C_{74}$,¹³ $\text{Ca}@C_{76}$,¹⁵ four isomers of $\text{Ca}@C_{82}$,^{16–18} two isomers of $\text{Ca}@C_{84}$,¹⁴ $\text{Ca}@C_{88}$,¹³ and two isomers of $\text{Ca}@C_{90}$.¹³ Here, we report the preparation, isolation, and structural characterization of a new calcium-containing endohedral $\text{Ca}@C_{3v}\text{-C}_{94}$. Endohedral fullerenes containing only a single metal ion are frequently encountered during the preparation of endohedrals of the trimetallic nitride, $\text{M}_3\text{N}@C_{2n}$, class. The incorporation of a number of different lanthanide ions into endofullerenes allows the preparation of molecules with a wide, but controllable, variation in properties and potential uses.^{19,20} For example, thulium compounds are luminescent and paramagnetic. Thus, there is current interest in using thulium compounds in developing new lasers²¹ and in magnetic resonance imaging contrast agents.²² The preparations and crystallographic characterization of the thulium-containing endohedrals, $\text{Tm}_3\text{N}@I_h\text{-C}_{80}$,²³ $\text{Tm}_3\text{N}@D_{5h}\text{-C}_{80}$, and $\text{Tm}_3\text{N}@C_s(51365)\text{-C}_{84}$,²⁴ have recently been reported. The procedure responsible for the formation of these thulium-containing trimetallic nitride endohedrals also produces $\text{Tm}@C_{3v}\text{-C}_{94}$. Here, we shall compare the properties and structures of $\text{Ca}@C_{3v}\text{-C}_{94}$ and $\text{Tm}@C_{3v}\text{-C}_{94}$.

Results

Preparation and Purification of $\text{Ca}@C_{3v}\text{-C}_{94}$. Carbon soot containing $\text{Ca}@C_{3v}\text{-C}_{94}$ was obtained by the direct current (DC) arc vaporization of graphite rods filled with CaO /graphite powder (1:80 atomic ratio). The soluble fullerenes were extracted from the soot, and two isomers, $\text{Ca}@C_{94}\text{(I)}$ and $\text{Ca}@C_{94}\text{(II)}$, were separated via multiple stages of chromatography. Relevant HPLC chromatograms from the purification process are shown in the Supporting Information. The major isomer was the more rapidly eluting $\text{Ca}@C_{94}\text{(I)}$ with a retention time of 27 min

(13) Wang, L. S.; Alford, J. M.; Chai, Y.; Diener, M.; Zhang, J.; McClure, S. M.; Guo, T.; Scuseria, G. E.; Smalley, R. E. *Chem. Phys. Lett.* **1993**, *207*, 354.

(14) Wan, T. S. M.; Zhang, H.-W.; Nakane, T.; Xu, Z.; Inakuma, M.; Shinohara, H.; Kobayashi, K.; Nagase, S. *J. Am. Chem. Soc.* **1998**, *120*, 6806.

(15) Zhang, Y.; Xu, J. X.; Hao, C.; Shi, Z. J.; Gu, Z. N. *Carbon* **2006**, *44*, 475.

(16) Xu, Z.; Nakane, T.; Shinohara, H. *J. Am. Chem. Soc.* **1996**, *118*, 11309.

(17) Slanina, Z.; Kobayashi, K.; Nagase, S. *J. Chem. Phys.* **2004**, *120*, 3397.

(18) Kodama, T.; Fujuu, R.; Miyake, Y.; Sakaguchi, K.; Nishikawa, H.; Ikemoto, I.; Kikuchi, K.; Achiba, Y. *Chem. Phys. Lett.* **2003**, *377*, 197.

(19) Dorn, H. C.; Iezzi, E. B.; Stevenson, S.; Balch, A. L.; Duchamp, J. C. In *Endofullerenes: A New Family of Carbon Clusters*; Akasaka, T., Nagase, S., Eds.; Kluwer: Dordrecht, 2002; pp 121–129.

(20) Dunsch, L.; Yang, S. *Small* **2007**, *3*, 1298.

(21) Voron'ko, Yu. K.; Zharikov, E. V.; Lis, D. A.; Popov, A. V.; Smirnov, V. A.; Subbotin, K. A.; Khromov, M. N.; Voronov, V. V. *Optics Spect.* **2008**, *105*, 538.

(22) Suchy, M.; Li, A. X.; Bartha, R.; Hudson, R. H. E. *Bioorg. Med. Chem.* **2008**, *16*, 6156.

(23) Zuo, T.; Olmstead, M. M.; Beavers, C. M.; Balch, A. L.; Wang, G.; Yee, G. T.; Shu, C.; Xu, L.; Elliott, B.; Echegoyen, L.; Duchamp, J. C.; Dorn, H. C. *Inorg. Chem.* **2008**, *47*, 5234.

(24) Zuo, T.; Walker, K.; Olmstead, M. M.; Melin, F.; Holloway, B. C.; Echegoyen, L.; Dorn, H. C.; Chaur, M. N.; Chancellor, C. J.; Beavers, C. M.; Balch, A. L.; Athans, A. J. *Chem. Commun.* **2008**, 1067.

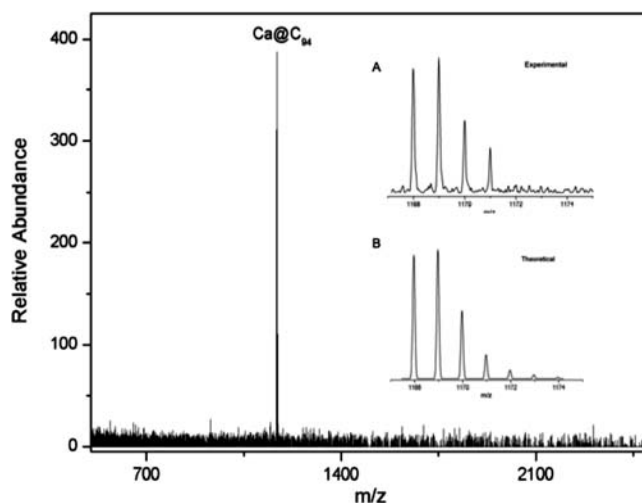


Figure 1. Laser desorption time-of-flight mass spectrum of $\text{Ca}@C_{3v}\text{-C}_{94}$. A, an expansion of the experimental spectrum. B, calculated isotope distributions for $\text{Ca}@C_{94}$.

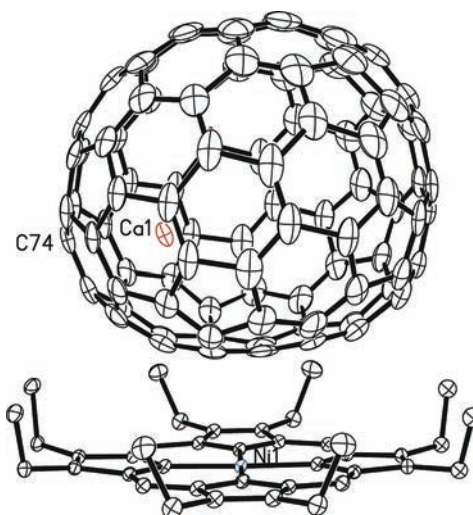


Figure 2. View showing the orientation of the endohedral $\text{Ca}@C_{3v}\text{-C}_{94}$ and the nickel porphyrin in crystalline $\text{Ca}@C_{3v}\text{-C}_{94}\text{-Ni(OEP)}\cdot 2(\text{CH}_3\text{C}_6\text{H}_5)$. Thermal ellipsoids are shown at the 50% level.

on a Buckyprep-M column with toluene as the mobile phase at flow rate of 4.5 mL/min. Insufficient quantities of the minor isomer, $\text{Ca}@C_{94}\text{(II)}$ with a retention time of 34 min under similar conditions, were obtained to allow crystallization and structural characterization. The mass spectrum of the purified $\text{Ca}@C_{94}\text{(I)}$ is shown in Figure 1. A sample of $\text{Ca}@C_{94}\text{(I)}$ was cocrystallized with Ni(OEP) and utilized in the crystallographic work. This procedure allowed us to identify $\text{Ca}@C_{94}\text{(I)}$ as $\text{Ca}@C_{3v}\text{-C}_{94}$.

Structure of $\text{Ca}@C_{3v}\text{-C}_{94}\text{-Ni(OEP)}\cdot 2(\text{CH}_3\text{C}_6\text{H}_5)$. Although there is disorder in this structure, the features of the major orientation are particularly well determined. In the major orientation, the cage resides with the crystallographic mirror plane coincident with one of the mirror planes of the endohedral fullerene. The total fractional occupancy of this orientation is 0.64. There is also one calcium ion site located on this mirror plane, and it, too, has 0.64 total occupancy. Figure 2 shows the relationship between the nickel porphyrin and the endohedral fullerene in the major orientation, while Figure 3 presents two orthogonal views $\text{Ca}@C_{3v}\text{-C}_{94}$ alone.

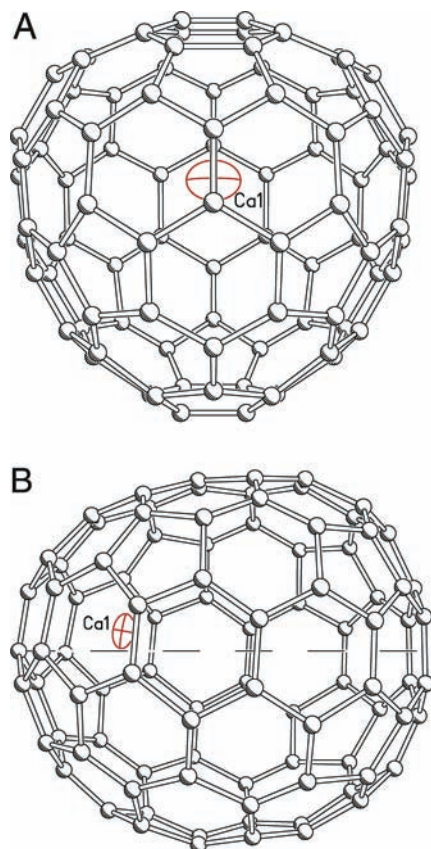


Figure 3. Two orthogonal views of $\text{Ca}@C_{3v}\text{-C}_{94}$. A, a view down the non-crystallographic 3-fold axis of the carbon cage. B, a side view with the 3-fold axis denoted by the horizontal, dashed line.

The crystallographic work clearly shows that the fullerene cage has C_{3v} symmetry. For a carbon cage with 94 atoms, there are 134 isomers that obey the isolated pentagon rule (IPR). Among these, only one, the one found in $\text{Ca}@C_{3v}\text{-C}_{94}$, has C_{3v} symmetry; all of the others have lower symmetry.

Remarkably, in the major orientation there is only a single position for the calcium ion, which is located over one of the 6:6 ring junctions that radiate from the C_3 axis. Figure 4 presents some details regarding the location of the calcium ion. The closest Ca–C distances are 2.358(8) and 2.445(7) Å. These distances are significantly shorter than the Ca–C distances in traditional calcium containing organometallic molecules. A search of the Cambridge Crystallographic Database reveals that the Ca–C distances in complexes containing the $\text{Ca}(\text{C}_5\text{H}_5\text{-}n\text{R}_n)_2$ fragment range from 2.574 to 2.865 Å with a mean distance of 2.678 Å. For example, in $(\eta^5\text{-C}_5\text{Me}_5)_2\text{Ca}$ the average Ca–C distance is reported to be 2.64(2) Å.²⁵ This shortening of the Ca–C distances in $\text{Ca}@C_{3v}\text{-C}_{94}$ may result from the unusual nature of the calcium ion coordination in $\text{Ca}@C_{3v}\text{-C}_{94}$. The calcium ion makes contact with the fullerene along one side only, the rest of the $[\text{C}_{94}]^{2-}$ ion is devoid of any interaction with the metal ion.

In addition to the major orientation, there are two other, symmetry-related minor orientations with 0.18 fractional occupancies for the cage. In these locations

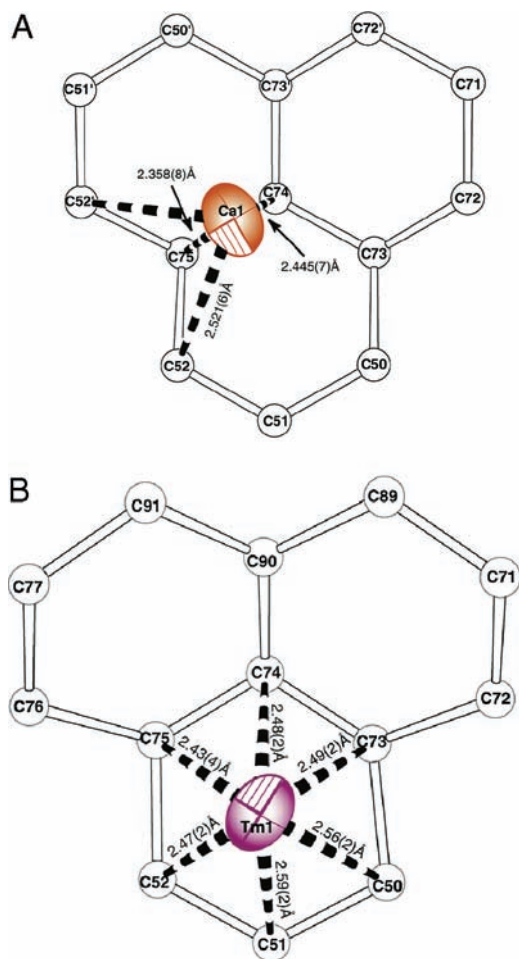


Figure 4. Drawings showing the location of the (A) calcium ion relative to the neighboring carbon atoms in $\text{Ca}@C_{3v}\text{-C}_{94}$ and (B) the thulium ion in $\text{Tm}@C_{3v}\text{-C}_{94}$.

the crystallographic mirror plane is not coincident with a mirror plane of the fullerene cage. Likewise, there are two other sites for the calcium ion on opposite sides of the mirror plane with 0.18 fractional occupancy of each site. As with the major orientation, the calcium ions in the minor orientations also lie over a pair of carbon atoms at a 6:6 ring junction of the cage.

Electronic Structure Computations for $\text{Ca}@C_{3v}\text{-C}_{94}$. The electronic distribution for calcium-containing endohedral fullerenes may be represented by an ionic model, $\text{Ca}^{2+} @(\text{C}_{2n})^{2-}$. This formulation requires that two electrons be transferred to the carbon cage. These electrons will fill the lowest unoccupied molecular orbital(s) (LUMOs) of the corresponding empty fullerene cage. Poblet and co-workers have proposed that the stability of various isomeric cages for a particular cage size can be estimated from computations of the empty cages. For endohedrals encapsulating $(\text{M}_3\text{N})^{6+}$ units, they proposed that a large (LUMO-4)-(LUMO-3) gap in the corresponding empty cage would provide a large highest occupied molecular orbital (HOMO)–LUMO gap in the corresponding hexa-anion.^{26,27} Similarly, the most stable

(26) Campanera, J. M.; Bo, C.; Poblet, J. M. *Angew. Chem., Int. Ed.* **2005**, *44*, 7230.

(27) Valencia, R.; Rodriguez-Fortea, A.; Poblet, J. M. *Chem. Commun.* **2007**, 4161.

(25) Williams, R. A.; Hanusa, T. P.; Huffman, J. C. *Organometallics* **1990**, *9*, 1128.

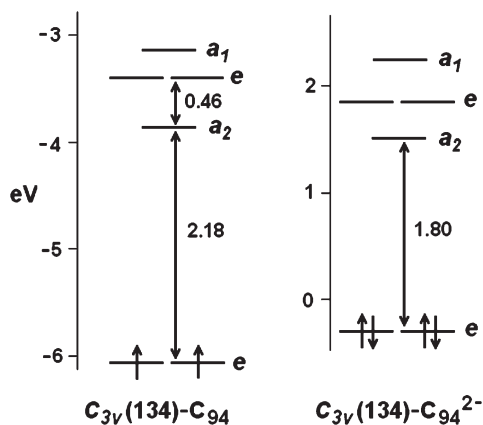


Figure 5. Molecular orbital energies (in eV) for neutral $C_{3v}\text{-}C_{94}$ and for the dianion, $[C_{3v}\text{-}C_{94}]^{2-}$.

Table 1. Relative Energies (ΔE , kJ/mol) and HOMO-LUMO Gaps (gap, eV) of the Most Stable Isomers of C_{94} , C_{94}^{2-} , and $\text{Ca}@C_{94}$

C_{94}^a			C_{94}^{2-a}			$\text{Ca}@C_{94}^d$		
cage	ΔE	gap ^b	cage	ΔE	gap ^b	cage	ΔE	gap
134: C_{3v}^c	5.8	2.18	124: C_2	0.0	1.56	134: C_{3v}	0.0	2.08
114: C_3^c	24.9	1.21	132: C_1	1.5	1.50	132: C_1	0.0	1.85
25: C_1	27.0	1.11	134: C_{3v}	2.8	1.80	118: C_1	8.2	1.38
124: C_2	1.2	1.10	118: C_1	3.8	1.39	122: C_1	9.7	1.40
24: C_{2v}	12.5	1.08	75: C_1	4.3	1.57	75: C_1	10.7	1.34
123: C_1	6.3	1.08	119: C_1	4.8	1.47	130: C_2	14.0	1.31
14: C_s	20.7	1.06	122: C_1	5.0	1.19	123: C_1	14.7	1.33
85: C_1	4.4	1.06	20: C_2	5.5	1.38	125: C_1	15.4	1.23
75: C_1	0.0	1.00	125: C_1	5.6	1.34	91: C_1	17.0	0.90
50: C_1	9.2	0.95	130: C_2	5.7	1.37	51: C_2	18.5	1.05

^a Computation at the DFT B3LYP/3-21G(d) level. ^b Gap = LUMO(2) – LUMO(1). ^c Triplet ground state. ^d Computation at the DFT B3LYP level, with the basis set of 3-21G for carbon and Lan12dz for calcium.

endohedral fullerene encapsulating $(M_2C_2)^{4+}$ units would be expected to have the largest (LUMO-3)-(LUMO-2) gap in the corresponding neutral fullerene.²⁸ Consequently, for $\text{Ca}@C_{94}$ we explored the magnitude of the (LUMO-2)-(LUMO-1) gaps for the empty cage C_{94} . Table 1 shows relevant computational results. The first column shows the 10 neutral C_{94} isomers with the largest (LUMO-2)-(LUMO-1) gaps. Of these ten, $C_{3v}\text{-}C_{94}$ has the largest gap. The molecular orbital energies for the frontier orbitals for $C_{3v}\text{-}C_{94}$, which has a triplet ground state, are shown in Figure 5 along with the orbital energies for the corresponding dianion. Computations were also performed to determine the relative stabilities of the dianions of the empty cage C_{94} , as done previously by Popov and Dunsch for other endohedrals.²⁹ Table 1 shows the values of ΔE and the HOMO-LUMO gaps for the 10 most stable anions. In this situation, the most stable isomer is $C_2(124)\text{-}C_{94}$. The $C_{3v}\text{-}C_{94}$ isomer is the third most stable, although it still has the largest HOMO-LUMO gap. Additional computations were conducted on the entire molecule. These were restricted to examination of the 15 cage geometries that produced the most stable dianions. The results are shown in the final columns of Table 1.

(28) Valencia, R.; Rodriguez-Fortea, A.; Poblet, J. M. *J. Phys. Chem. A* **2008**, *112*, 4550–4555.

(29) Popov, A. A.; Dunsch, L. *J. Am. Chem. Soc.* **2007**, *129*, 11835–11849.

The $C_{3v}\text{-}C_{94}$ isomer emerges as the most stable, but the $C_1(132)\text{-}C_{94}$ isomer is very close in energy, only 0.002 eV less stable.

Preparation and Purification of $\text{Tm}@C_{3v}\text{-}C_{94}$. Core-drilled graphite rods packed with a mixture of Tm_2O_3 , graphite powder, and iron nitride were vaporized in Krätschmer-Huffman arc-discharge fullerene generator as described previously.³⁰ Extraction procedures and chromatographic purification, utilizing a cyclopentadiene functionalized Merrifield peptide resin column,³¹ also followed an established route.^{18,19} Figure 6 shows the mass spectrum of the purified product.

Figure 7 shows the UV/vis absorption spectra of $\text{Ca}@C_{3v}\text{-}C_{94}$ and $\text{Tm}@C_{3v}\text{-}C_{94}$. The two spectra show some general similarity but also a number of distinct differences. The spectrum of $\text{Tm}@C_{3v}\text{-}C_{94}$ in particular is very similar to the spectrum reported previously for $\text{Yb}@C_{94}$,³² and these two endohedral fullerenes are likely to have the same structure.

Structure of $\text{Tm}@C_{3v}\text{-}C_{94} \cdot 2\text{Ni(OEP)} \cdot 3.65(\text{C}_6\text{H}_6)$. Unlike all of the other endohedral fullerenes that have been cocrystallized with Ni(OEP), $\text{Tm}@C_{3v}\text{-}C_{94}$ forms crystals with a stoichiometry of two molecules of Ni(OEP) to one molecule of $\text{Tm}@C_{3v}\text{-}C_{94}$, rather than the usual stoichiometry of one molecule of the endohedral and one molecule of Ni(OEP).³³ As a result, each molecule of $\text{Tm}@C_{3v}\text{-}C_{94}$ is surrounded by two molecules of Ni(OEP) as can be seen in Figure 8. This view shows the major orientation of the C_{94} cage and the three most abundant sites for the Tm ion. As is the case with the calcium endohedral, this thulium endohedral utilizes the unique C_{94} isomer with C_{3v} symmetry. The two different porphyrin molecules exhibit different interactions with the fullerene. Both porphyrin molecules have low average deviations from planarity, as measured from the NiN_4 plane, but the porphyrin containing Ni1 is slightly more planar. This porphyrin interacts with a relatively flat face of the endohedral fullerene. The porphyrin containing Ni2 interacts with a more pyramidalized area of the fullerene, and has the shorter NiN_4 plane-to-ball distance, 2.855(3) Å.

Figure 9 shows two orthogonal views of $\text{Tm}@C_{3v}\text{-}C_{94}$ with the three major sites for the Tm ions shown. The C_{94} cage is disordered. Two orientations with occupancies of 0.5 and 0.4 were identified and refined. A third minor orientation may be present, but the data were insufficient to allow it to be modeled. In addition to the three major sites for Tm ions, there are several sites with less than 0.1 occupancy. In the major cage orientation, the Tm ions are situated over the centers of six-membered rings as can be seen in Figure 4 for Tm1. Similar situations pertain for Tm2 and Tm3. This orientation of Tm ions over six-membered rings has been seen before for $\text{Tm}_3\text{N}@I_h\text{-}C_{80}$.¹⁸

(30) Zuo, T.; Olmstead, M. M.; Beavers, C. M.; Balch, A. L.; Wang, G.; Yee, G. T.; Shu, C.; Xu, L.; Elliot, B.; Echegoyen, L.; Duchamp, J. C.; Dorn, H. C. *Inorg. Chem.* **2008**, *47*, 5234.

(31) Ge, Z.; Duchamps, J. C.; Cai, T.; Gibson, H. W.; Dorn, H. C. *J. Am. Chem. Soc.* **2005**, *127*, 16292.

(32) Xu, J.; Wang, Z.; Shi, Z.; Gu, Z. *Chem. Phys. Lett.* **2005**, *409*, 192.

(33) However, C_{60} does form cocrystals with a 2:1, porphyrin/ C_{60} stoichiometry: $C_{60} \cdot 2\text{Co}^{\text{II}}(\text{OEP}) \cdot \text{CHCl}_3$ and $C_{60} \cdot 2\text{Zn}^{\text{II}}(\text{OEP}) \cdot \text{CHCl}_3$. Olmstead, M. M.; Costa, D. A.; Maitra, K.; Noll, B. C.; Phillips, S. L.; Van Calcar, P. M.; Balch, A. L. *J. Am. Chem. Soc.* **1999**, *121*, 7090.

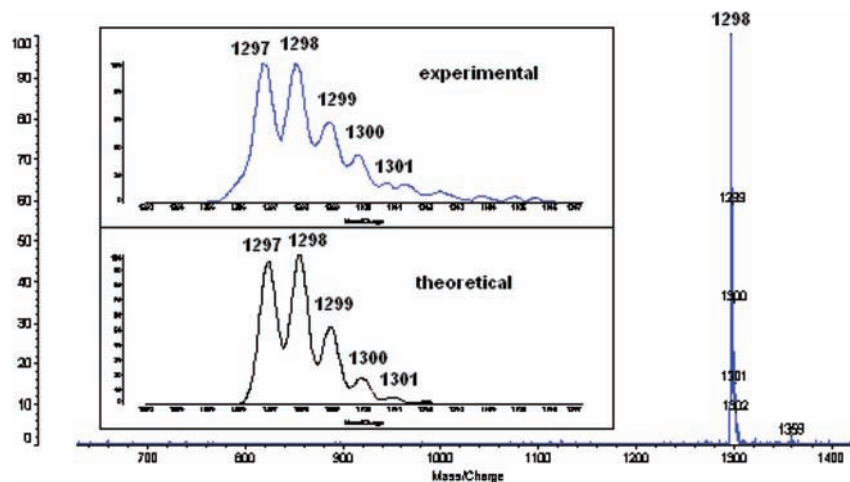


Figure 6. Negative ion mode LD-TOF mass spectrum of the pure $\text{Tm}@C_{3v}\text{-C}_{94}$. The inset panel is the experimental and theoretical isotopic distribution of $\text{Tm}@C_{3v}\text{-C}_{94}$.

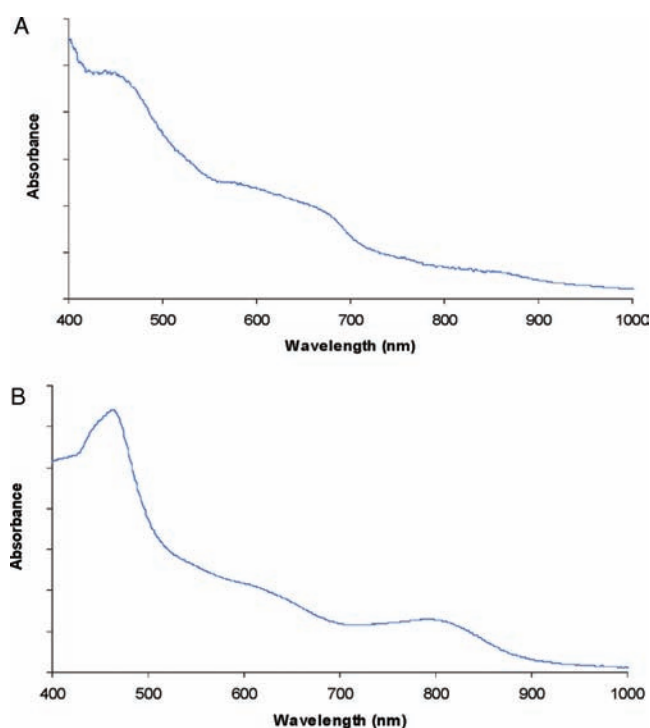


Figure 7. Absorption spectra. (A) $\text{Ca}@C_{3v}\text{-C}_{94}$ in benzene solution. (B) $\text{Tm}@C_{3v}\text{-C}_{94}$ in toluene solution.

To allow appreciation of the size of the $C_{3v}\text{-C}_{94}$ cage, Figure 10 shows drawings of C_{60} in $C_{60}\cdot 2\text{Zn}^{\text{II}}(\text{OEP})\cdot \text{CHCl}_3$ ²³ and $\text{Tm}@C_{3v}\text{-C}_{94}$ in crystalline $\text{Tm}@C_{3v}\text{-C}_{94}\cdot 2\text{Ni}(\text{OEP})\cdot 3.65(\text{C}_6\text{H}_6)$ on the same scale. The larger size of $\text{Tm}@C_{3v}\text{-C}_{94}$ is readily apparent.

Discussion

At this time, $\text{Ca}@C_{3v}\text{-C}_{94}$ and $\text{Tm}@C_{3v}\text{-C}_{94}$ are the largest fullerenes that have been characterized by single crystal X-ray diffraction. Both obey the IPR. In each of these molecules, the preferred sites for the metal ions are positions near the site where the 3-fold axis intersects the fullerene surface at a rather curved end. However, while the calcium ion prefers to lie above a single C–C bond, the thulium ion resides over a six-membered ring. This localization of the metal ions leaves a considerable amount of empty space, about 70 \AA^3 ,

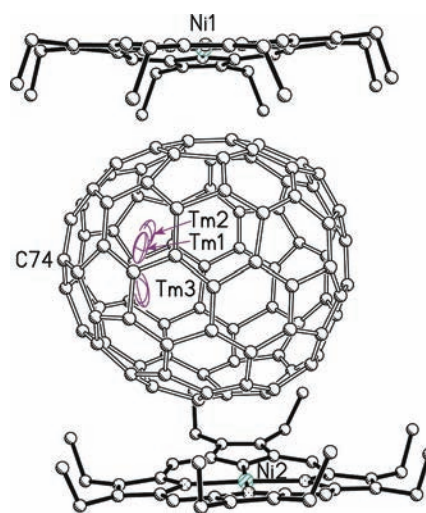


Figure 8. View showing the orientation of the endohedral $\text{Tm}@C_{3v}\text{-C}_{94}$ and the two nickel porphyrins in crystalline $\text{Tm}@C_{3v}\text{-C}_{94}\cdot 2\text{Ni}(\text{OEP})\cdot 3.65(\text{C}_6\text{H}_6)$. The fractional occupancies of the three Tm sites are Tm1, 0.40; Tm2, 0.26; and Tm3, 0.21. For clarity, the hydrogen atoms are not shown, and all atoms are represented as uniform, arbitrarily sized circles.

on the other side of the cage. In contrast to the $\text{M}_3\text{N}@C_{2n}$ class of endohedrals, in which the internal cluster geometry partially dictates the relative positions of the metal and carbon atoms, the $\text{M}@C_{2n}$ class, with its internal simplicity, offers fewer constraints on the positioning of the metal atom. The localization of the metal ions seen for $\text{Ca}@C_{3v}\text{-C}_{94}$ and $\text{Tm}@C_{3v}\text{-C}_{94}$ also contrasts markedly with the metal ion placement in $\text{Er}@C_{2v}\text{-C}_{82}$ where there are 23 partially occupied sites for the erbium ions³⁴ and in $\text{Er}@C_{3v}(8)\text{-C}_{82}$ where there are also erbium ions in 23 fractionally populated positions.³⁵

The similarities in the structures of these two endohedral fullerenes suggest that they may have similar electronic structures. For $\text{Ca}@C_{3v}\text{-C}_{94}$, an ionic structure $\text{Ca}^{2+}[\text{C}_{94}]^{2-}$ is expected and has been utilized in our computational studies. For $\text{Tm}@C_{3v}\text{-C}_{94}$ the alternative structures are $\text{Tm}^{2+}[\text{C}_{94}]^{2-}$ or $\text{Tm}^{3+}[\text{C}_{94}]^{3-}$. Compounds

(34) Olmstead, M. M.; de Bettencourt-Dias, A.; Stevenson, S.; Dorn, H. C.; Balch, A. L. *J. Am. Chem. Soc.* **2002**, *124*, 4172.

(35) Olmstead, M. M.; Lee, H. M.; Stevenson, S.; Dorn, H. C.; Balch, A. L. *Chem. Commun.* **2002**, 2688.

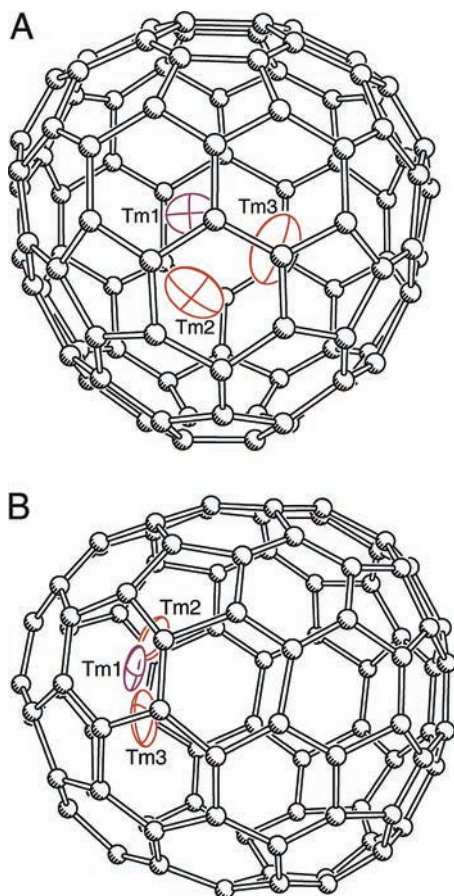


Figure 9. Two orthogonal views of $\text{Tm}@C_{3v}\text{-C}_{94}$. A, a view down the non-crystallographic 3-fold axis of the carbon cage. B, a side view with the 3-fold axis in the horizontal direction. The major Tm site is shown in orange, while the other two prominent sites are pink.

containing Tm^{2+} are now known for organometallic complexes^{36–38} and also for endohedral fullerenes.³⁹ As an example of the latter, the three isomers of $\text{Tm}@C_{82}$ have been formulated with the electronic distribution, $\text{Tm}^{2+}[\text{C}_{82}]^{2-}$.^{40,41} For $\text{Tm}@C_{3v}\text{-C}_{94}$, the use of the same $C_{3v}\text{-C}_{94}$ cage structure as found for the calcium compound suggests that the $\text{Tm}^{2+}[\text{C}_{94}]^{2-}$ electronic distribution is probable. However, the differences in the electronic spectra of $\text{Tm}@C_{3v}\text{-C}_{94}$ and $\text{Ca}@C_{3v}\text{-C}_{94}$ seen in Figure 6 and the different metal ion placements seen in Figure 4 suggest that the alternative formal electronic distribution, $\text{Tm}^{3+}[\text{C}_{94}]^{3-}$, may contribute to a larger extent than is the case for $\text{Ca}@C_{3v}\text{-C}_{94}$.

Given the 134 IPR isomers available for a C_{94} cage and the possibility that a non-IPR cage could form as well, we find it remarkable that the procedures reported here for making $\text{Ca}@C_{3v}\text{-C}_{94}$ and $\text{Tm}@C_{3v}\text{-C}_{94}$ lead to the formation of the same cage isomer for both molecules.

(36) Evans, W. J.; Allen, N. T.; Ziller, J. W. *Angew. Chem., Int. Ed.* **2002**, *41*, 359.

(37) Jaroschik, F.; Nief, F.; Le Goff, X. F.; Ricard, L. *Organometallics* **2007**, *26*, 3552.

(38) Bochkarev, M. N. *Coord. Chem. Rev.* **2004**, *248*, 835.

(39) Hino, S.; Wanita, N.; Iwasaki, K.; Yoshimura, D.; Ozawa, N.; Kodama, T.; Sakaguchi, K.; Nishikawa, H.; Ikemoto, I.; Kikuchi, K. *Chem. Phys. Lett.* **2005**, *402*, 217.

(40) Kirbach, U.; Dunsch, L. *Angew. Chem., Int. Ed. Engl.* **1996**, *35*, 2380.

(41) Kodama, T.; Ozawa, N.; Miyake, Y.; Sakaguchi, K.; Nishikawa, H.; Ikemoto, I.; Kikuchi, K.; Achiba, Y. *J. Am. Chem. Soc.* **2002**, *124*, 1452.

Experimental Section

Synthesis of $\text{Ca}@C_{3v}\text{-C}_{94}$. A 6×150 mm graphite rod filled with CaO /graphite powder (1:80 atomic ratio) was vaporized as the anode in a DC arc under optimized conditions.⁴² The raw soot that resulted was extracted repeatedly in *o*-dichlorobenzene with ultrasonication until the extract solution was colorless, without special nitrogen protection. After removing the solvent with a rotary evaporator, chlorobenzene was added to redissolve the dry powder. The extract was subjected to a four-stage HPLC isolation process that did not involve recycling.

The first, second, and third steps were carried out on three complementary columns Buckyprep-M (with chlorobenzene as eluent), Buckyprep (with toluene as eluent) and 5PBB (10×250 mm Nacalai Tesque, with xylene as eluant) at a flow rate of 4.5 mL/min. The final stage, which produced isomer-free $\text{Ca}@C_{94}$, utilized a Buckyprep-M column with toluene as eluent.

The purity and composition of $\text{Ca}@C_{94}$ was determined by laser desorption time-of-flight mass spectrometry (LD-TOF-MS). UV-4100 spectrophotometer (Hitachi High-Technologies Corporation) was used to characterize its ultraviolet–visible–near-infrared (UV–vis–NIR) spectrum in benzene solvent.

Synthesis of $\text{Tm}@C_{3v}\text{-C}_{94}$. The core-drilled graphite rods (6.5 mm dia.) were packed with a mixture of Tm_2O_3 , graphite powder, and iron nitride according to weight ratio of 2.1:1.0:0.4, respectively, and vaporized in Krätschmer–Huffman arc-discharge fullerene generator as described previously. The fullerene containing soot was collected in a thimble and extracted in a Soxhlet extractor using toluene as solvent for about 20 h. The first stage of HPLC of the flash eluant from the chemical separation using a cyclopentadiene-functionalized Merrifield peptide resin (CPDE-MPR) revealed the presence of seven thulium-containing fractions on 5PBB column, similar to those of the terbium-based elution using same method. The sixth fraction contained $\text{Tm}@C_{94}$ and $\text{Tm}_3\text{N}@C_{88}$. A pure sample of $\text{Tm}@C_{94}$ was obtained from the second stage of HPLC using a 5PYE column.

Crystal Growth. Cocrystals of $\text{Tm}@C_{3v}\text{-C}_{94}$ and $\text{Ni}^{\text{II}}(\text{OEP})$ were obtained by layering a solution of about 0.5 mg of $\text{Tm}@C_{3v}\text{-C}_{94}$ in 0.5 mL benzene over a red benzene solution of $\text{Ni}^{\text{II}}(\text{OEP})$ in a glass tube. Over a 14 day period, the two solutions diffused together and black crystals formed. Cocrystals of $\text{Ca}@C_{3v}\text{-C}_{94}$ and $\text{Ni}^{\text{II}}(\text{OEP})$ were obtained by layering a saturated solution of $\text{Ni}^{\text{II}}(\text{OEP})$ in 0.5 mL of toluene over a toluene solution of $\text{Ca}@C_{3v}\text{-C}_{94}$ in a glass tube.

$\text{Tm}@C_{3v}\text{-C}_{94} \cdot 2 \text{Ni}(\text{OEP}) \cdot 3.65\text{C}_6\text{H}_6$. A black needle of dimensions $0.12 \times 0.03 \times 0.02$ mm was mounted in the 90(2) K nitrogen cold stream provided by an Oxford Cryostream low temperature apparatus on the goniometer head of a Bruker D85 diffractometer equipped with an ApexII CCD detector, on beamline 11.3.1 at the Advanced Light Source in Berkeley, CA. Diffraction data were collected using synchrotron radiation monochromated with silicon(111) to a wavelength of 0.77490(1). A full sphere of data was collected using 0.3° ω scans. A multiscan absorption correction was applied using the program SADABS 2007/4.⁴³ Upon inspection of scattering intensities, the data were truncated to 1 Å resolution, yielding 125844 reflections collected, of which 11978 were unique [$R(\text{int}) = 0.0944$] and 10015 were observed [$I > 2\sigma(I)$]. The structure was solved by dual-space methods (SIR-2004)⁴⁴ and refined by full-matrix least-squares on F^2 (SHELXL97)³¹ using 1246 parameters. The experimental crystal is a merohedral twin that was

(42) Sun, D.-Y.; Liu, Z.-Y.; Guo, X.-H.; Xu, W.-G.; Liu, S.-Y. *J. Phys. Chem. B* **1997**, *101*, 3927.

(43) Sheldrick, G. M. *Acta Crystallogr., Sect. A* **2008**, *64*, 112.

(44) Burla, M. C.; Camalli, M.; Carrozzini, B.; Cascarano, G. L.; Giacovazzo, C.; Polidori, G.; Spagna, R. *J. Appl. Crystallogr.* **2003**, *36*, 1103.

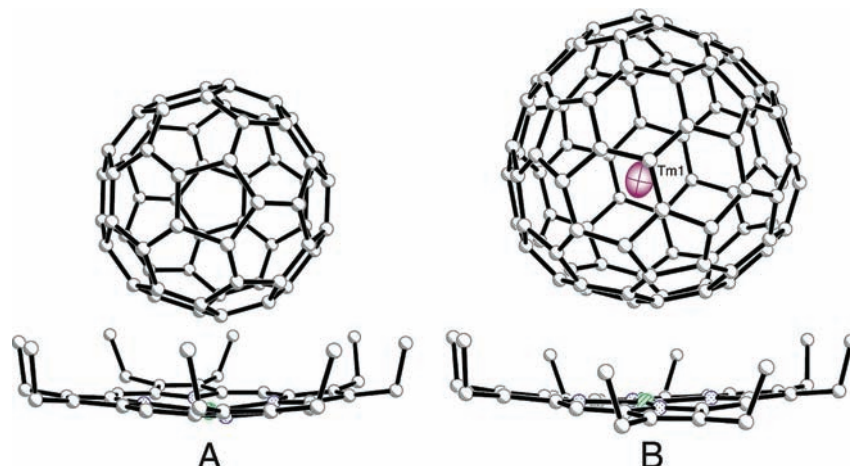


Figure 10. Drawings comparing the sizes of (A) C_{60} in $C_{60} \cdot 2Zn^{II}(OEP) \cdot CHCl_3$ and (B) $Tm@C_{3v}-C_{94}$ in crystalline $Tm@C_{3v}-C_{94} \cdot 2Ni(OEP) \cdot 3.65(C_6H_6)$ with only the major Tm site shown. Only one porphyrin is shown for each structure.

treated using a 180° rotation about $[1\ 1\ 0]$. This treatment yielded a twin ratio of 52:48.

The C_{94} cage is disordered. Two orientations were identified and refined. The occupancies of these two cages were 0.5 and 0.4. At least one more orientation was present, but could not be modeled because of a deficit of data. Because of the overlap of cage orientations, distance restraints were used to control the cage geometries. The thulium atom within the C_{94} cage is disordered over numerous sites. Occupancies were initially determined by refinement and were subsequently fixed at their refined values. The structure was refined primarily isotropically because of the low data to parameter ratio. Only the thulium sites Tm1, Tm2, and Tm3 with occupancies of 0.40, 0.26, and 0.21, respectively, were refined anisotropically. The other thulium sites, which had occupancies less than 0.10, were refined isotropically. The hydrogen atoms on carbon atoms were generated geometrically and refined as riding atoms with $C-H = 0.95-0.99\ \text{\AA}$ and $U_{iso}(H) = 1.2$ times $U_{eq}(C)$ for CH and CH_2 groups and $U_{iso}(H) = 1.5$ times $U_{eq}(C)$ for CH_3 groups. The maximum and minimum peaks in the final difference Fourier map were 2.013 and $-0.676\ e\text{\AA}^{-3}$. The maximum lies on a special position, and is probably an artifact of the twinning. Crystal data: $C_{181}H_{103}N_8Ni_2Tm$, $M_w = 2676.01$, tetragonal, $I4_1/a$, $a = 25.672(4)\ \text{\AA}$, $b = 25.672(4)\ \text{\AA}$, $c = 69.62(2)\ \text{\AA}$, $V = 45884(17)\ \text{\AA}^3$, $T = 90(2)\ \text{K}$, $Z = 16$, $R_1 [I > 2\sigma(I)] = 0.0934$, wR_2 (all data) = 0.2539, GOF (on F^2) = 1.035.

$Ca@C_{3v}-C_{94} \cdot Ni(OEP) \cdot 2(CH_3C_6H_5)$. A black block of dimensions $0.24 \times 0.34 \times 0.46\ \text{mm}$ was mounted in the 91(2) K nitrogen cold stream provided by Cryo Industries low temperature apparatus on the goniometer head of a Bruker SMART diffractometer equipped with an ApexII CCD detector. Data were collected with the use of $Mo\ K\alpha$ radiation ($\lambda = 0.71073\ \text{\AA}$). A multiscan absorption correction was applied using the program SADABS 2008/1.³¹ A total of 56378 reflections were collected to $2\theta_{max}$ of 61° , of which 12968 were unique [$R(int) = 0.0238$] and 10427 were observed [$I > 2\sigma(I)$]. The structure was solved by direct methods (SHELXS97) and refined by full-matrix least-squares on F^2 (SHELXL97) using 1997 parameters.³¹ There are two orientations of the C_{94} cage in the structure. The first residue contains 51 C atoms, of which 8 reside on the crystallographic mirror plane. The second contains 94 C atoms, which comprise a ball that is disordered with respect to the crystallographic mirror plane.

The coordinates of the second cage were adjusted by a rigid group refinement. This group was taken from the atoms (including those generated by symmetry) of the first cage. The major orientation is the first cage, with refined occupancy of 0.3204(15); the second cage has occupancy of 0.1796(15). There are two Ca atoms in the asymmetric unit, and because of their refined occupancies and positions, Ca1 was associated with the first ball and Ca2 was associated with the second. Ca1 was refined with anisotropic thermal parameters and Ca2 was kept isotropic. Carbon atoms of the first cage were refined with anisotropic thermal parameters while those of the second cage were kept isotropic. Similarity restraints of $0.02\ \text{\AA}$ were applied to the thermal parameters of the carbon cages and the two Ca atoms. There are two toluene sites in the structure, and they also exhibit some disorder with a total of 0.5 occupancy in each of the two sites.

The hydrogen atoms on carbon atoms were treated as for the Tm structure. The maximum and minimum peaks in the final difference Fourier map were 1.494 and $-1.510\ e\ \text{\AA}^{-3}$. Crystal data: $C_{144}H_{60}CaN_4Ni$, $M_w = 1944.75$, monoclinic, $C2/m$, $a = 25.740(5)\ \text{\AA}$, $b = 15.106(3)\ \text{\AA}$, $c = 21.320(4)\ \text{\AA}$, $\beta = 96.77(3)^\circ$, $V = 8232(3)\ \text{\AA}^3$, $T = 91(2)\ \text{K}$, $Z = 4$, $R_1 [I > 2\sigma(I)] = 0.0824$, wR_2 (all data) = 0.2521, GOF (on F^2) = 1.035.

Acknowledgment. We thank the National Science Foundation [CHE-0716843 to A.L.B. and M.M.O., CHE-0443850 (H.C.D.), DMR-0507083 (H.C.D.)] and the National Institute of Health [1R01-CA119371-01 (H.C.D.)] for support, the Advanced Light Source, supported by the Director, Office of Science, Office of Basic Energy Sciences, of the U.S. Department of Energy under Contract No. DE-AC02-05CH11231, for beam time, and Dr. Simon J. Teat for assistance. We thank Zhejiang Sci-Tech University, Hangzhou, China for the mass spectrometry determinations. Hua Yang thanks Mudanjiang Normal College, Heilongjiang, China, for admission to full time graduate study.

Supporting Information Available: The HPLC chromatograms, UV-vis, and MS spectra of the purified samples of $Ca@C_{3v}-C_{94}$ and $Tm@C_{3v}-C_{94}$. X-ray crystallographic files in CIF format for $Ca@C_{3v}-C_{94} \cdot Ni(OEP) \cdot 2(CH_3C_6H_5)$ and $Tm@C_{3v}-C_{94} \cdot 2Ni(OEP) \cdot 3.65(C_6H_6)$. This material is available free of charge via the Internet at <http://pubs.acs.org>.